J Musculoskelet Neuronal Interact 2011; 11(3):243-248

Original Article

Hylonome

# An open source approach for regional cortical bone mineral density analysis

**T. Rantalainen[1,2,3,4], R. Nikander[1,5,6], A. Heinonen[3], R.M. Daly[1], H. Sievänen[6,7]**

[1]Centre for Physical Activity and Nutrition Research, School of Exercise and Nutrition Sciences, Deakin University, Melbourne; [2]Department of Mechanical engineering, Lappeenranta University of Technology, Finland; [3]Department of Health Sciences, University of Jyväskylä, Finland; [4]Neuromuscular Research Center, Department of Biology of Physical Activity, University of Jyväskylä, Finland; [5]Helsinki Metropolia University of Applied Sciences, Helsinki, Finland; [6]Pirkanmaa Hospital District, Science Center, Tampere, Finland; [7]Bone Research Group, UKK Institute, Tampere, Finland

**Abstract**

**Objective:** Cortical porosity, particularly at the endocortical region, is recognised to play a central role in the pathogenesis of bone fragility. Therefore, the purpose of this study was to: 1) demonstrate how cortical volumetric BMD (vBMD) distribution can be analysed from (p)QCT images and 2) highlight the clinical significance of assessing regional density distribution of cortical bone. **Methods:** We used pQCT to compare mid-tibial cortical volumetric BMD distribution of 20 young (age 24(SD2) years, mass 77(11) kg, height 178(6) cm) and 25 elderly (72(4) years, 75(9) kg, 172(5) cm) men. Radial and polar cortical vBMD distributions were analysed using a custom built open source analysis tool which allowed the cortex to be divided into three concentric cortical divisions and in 36 cortical sectors originating from the centroid of the bone. **Results:** Mean vBMD did not differ between the groups (1135(16) vs. 1130(28) mg/cm, P=0.696). In contrast, there was a significant age-group by radial division interaction for radial cortical vBMD (P<0.001). **Conclusions:** The proposed analysis method for analysing cortical bone density distribution of pQCT images was effective for detecting regional differences in cortical density between young and elderly men, which would have been missed by just looking at mean vBMD values.

**Keywords:** pQCT, Analysis, Image, Bone, Tibia

## Introduction

The age-related loss in cortical bone is recognised to play a central role in the pathogenesis of bone fragility. After the age of 65 years, most bone loss at appendicular sites is cortical and not trabecular and the cortical bone loss is associated with increasing cortical porosity[1]. However, cortical porosity is not distributed evenly throughout the cortex. For example,the endosteum appears to be more porous than the periosteum[1-3]. Furthermore, changes in cortical porosity with aging also varies throughout the cortex. Zebaze et al.[1] reported that 47% of cortical bone loss at the distal radius was due to intracortical remodelling (increased porosity) of the cortex adjacent to marrow, with a further 21% attributed to increased porosity in the remaining cortex. Therefore, developing a readily accessible tool to quantify (or estimate) the distribution of cortical density within the cortex will enhance our understanding of the pathogenesis of fractures and the role of pharmacological and lifestyle interventions to optimise bone strength.

Peripheral quantitative computed tomography (pQCT) is a common research tool to investigate skeletal rigidity[4]. Although cortical vBMD measured by (p)QCT only represents the apparent mineral density of cortical bone (i.e. porosity, mineralization[5-7]), there is experimental data indicating that it is strongly related to cortical porosity. Indeed, it has been reported that about 70% of the age-related reduction in cortical vBMD is due to increased porosity[6], which suggests that apparent vBMD of the cortex would provide an adequate surrogate of cortical porosity[8].

Therefore, the purpose of this study was to: 1) demonstrate how cortical volumetric BMD distribution can be analysed

The authors have no conflict of interest.

*Corresponding author: Timo Rantalainen, School of Exercise and Nutrition Sciences, Deakin University, 221 Burwood Highway, Burwood, VIC, 3125, Australia*
*E-mail: timo.rantalainen@deakin.edu.au*

*Edited by: J. Rittweger*
*Accepted 14 July 2011*

from (p)QCT images and 2) highlight the clinical significance of assessing regional density distribution of cortical bone. A key focus of the paper is to provide a detailed description of a method for regional cortical density distribution analysis of pQCT scans, discuss the advantages of the regional analysis and offer the regional analysis software for scientists as an open source tool.

## Methods

Analysis of cortical volumetric bone density (vBMD, mg/cm$^3$) distribution from quantitative tomographic images comprises three steps: 1) reading the data from the file and scaling the values to vBMD values, 2) segmenting bone and selecting a region of interest and 3) calculating the density distribution within the bone envelope. pQCT images measured with the Stratec XCT2000 device (Stratec Medizintechnik GmbH, Pforzheim, Germany) are used as examples in this paper.

*Step 1: Reading data*

The data in Stratec pQCT files is stored as signed 16-bit integers in little-endian byte order (i.e. least significant byte first) and the stored numbers denote linear attenuation coefficients (in units of 1/cm) multiplied by 1000. The attenuation coefficients are stored after a 1609 byte header containing patient specific information. In case of reading standardized DICOM files (http://medical.nema.org/) produced by clinical QCT devices, the data storage format can be found from the header. To scale the attenuation coefficients to volumetric density values of bone, the scaling equation needs to be determined either by using calibration samples of known $K_2HPO_4$ phantoms and obtaining the scaling equation from a linear fit obtained with least squares method[4] or by asking the manufacturer to offer the scaling equation. If the equation is supplied by the manufacturer, one may not know the exact details of how the equation has been derived and therefore using proper calibration phantoms could be considered the preferred way. After scaling the image, it is usually preprocessed[9]. A commonly used 3x3 median filter was applied in this study.

*Step 2: Segmenting bone and selecting region of interest*

Bone may be differentiated from surrounding soft tissues by simply applying a density threshold to the image. A suitable and common threshold value used for vBMD analysis is the mean between the soft tissue and the bone, i.e. 700 mg/cm$^3$ [10-12] and 690 mg/cm$^3$ was used in the present application. For tibial mid-shaft cross-sectional images, the tibia and fibula are visible in the same slice and therefore, the region of interest for the bone of interest needs to be defined. In the present application, the outer edges of continuous pixel groups were traced (i.e., the apparent periosteal boundaries of bones) after applying the threshold on the image. Then, the pixel group representing the longest traced edge was chosen as the region of interest. In the present study, the selected region of interest was the tibia in all cases. However, this simple method may fail if the cortex of the smaller bone is not continuous, which in practice nearly doubles the length of the traced edge. We have noticed that this misclassification can occur when analyzing data from older adults with low vBMD values and thin cortices. Also, this simple approach most likely does not apply to forearm bones with similar circumferences.

*Step 3: Calculating the polar and radial density distributions*

To eliminate partial volume effects[10,13], the outermost and innermost rows of cortical pixels are first peeled off by eroding the image by one pixel. The original image is in Cartesian coordinate system (i.e. x- and y-coordinates) but the polar coordinate system (i.e. r- and $\theta$-coordinates) was used for the density distribution determination. The area center of gravity of the bone marrow region (i.e., the area inside the innermost cortical boundary) was chosen as the origin of the polar coordinate system. The endocortical and pericortical radii were thereafter determined with 1° increments of $\theta$. The vBMD values were converted from the Cartesian to the polar coordinate system as:

$$vBMD(r,\theta) = vBMD(rounddown(X_{origin}+rcos\theta), rounddown(Y_{origin}+rsin\theta)) \quad (1)$$

For a given angle the radius was first set to zero. Thereafter the r was incremented with 1/10$^{th}$ of the planar resolution until the first cortical bone pixel was found. This radius was defined as the endocortical radius. Next the r was further incremented until no further bone pixels were detected and the r at that time was defined as the pericortical radius. While the radius was being incremented between the endocortical and pericortical border, the vBMD values corresponding to each intermediate radii were saved to a vBMD process. One vBMD process of varying length was thus created for each of the 360 1° increments of $\theta$.

The cortical cross-section was then divided into desired number of polar sectors and cortical radial divisions (Figure 1). Thirty six sectors and three divisions were used in the present study. Mean cortical polar volumetric bone mineral density (vBMD, mg/cm$^3$) was calculated in all radial divisions and within each sector from the vBMD process vector as follows:

$$vBMD_{k,l} = \frac{\sum_{\theta=(l-1)*360/sectors+1}^{l*360/sectors} \sum_{j=\frac{k-1}{divisions}*n_\theta+1}^{\frac{k}{divisions}*n_\theta} vBMD_{\theta,j}}{\sum_{\theta=(l-1)*360/sectors+1}^{l*360/sectors} n_\theta} \quad (2)$$

where k= index of radial division (from 1 to 3 in the present study), l = index of polar sector (from 1 to 36 in the present study), $\theta$= index of $\theta$ increment, $n_\theta$= length of the $\theta^th$ vBMD process, j = the index of radius increment, $vBMD_{\theta,j}$= value of the vBMD process vector at $\theta$,j.

Thereafter, the mean k$^{th}$ radial division vBMD was calculated as:

$$vBMD_k = \frac{\sum_{l=1}^{36} vBMD_{k,l}}{36} \quad (3)$$

Similarly, the mean l$^{th}$ polar sector vBMD for cortical bone was calculated as:

$$vBMD_l = \frac{\sum_{k=1}^{3} vBMD_{k,l}}{3} \quad (4)$$

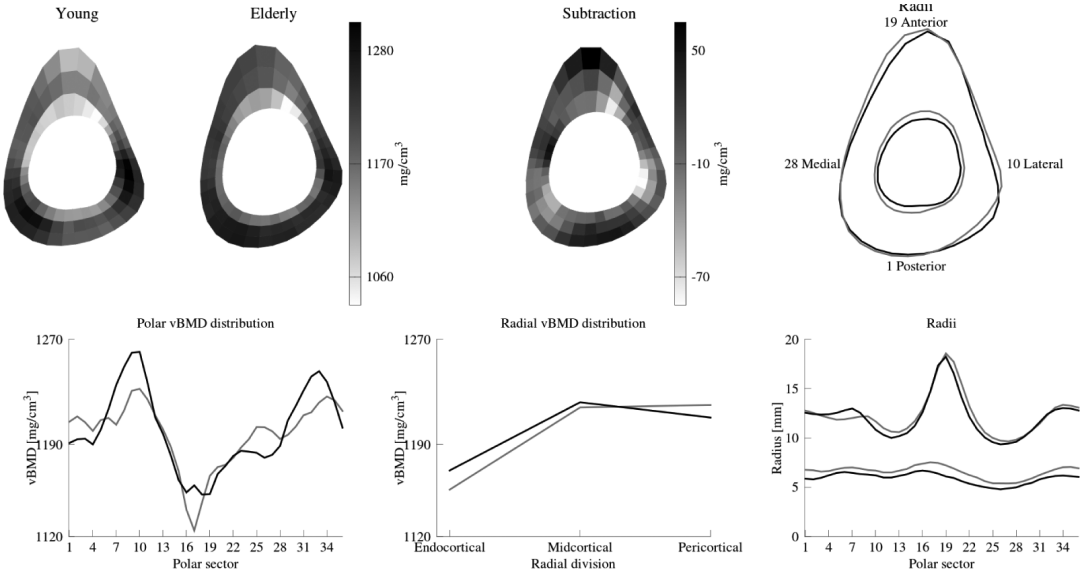


**Figure 1.** Polar (36 sectors) and radial (three concentric rings) vBMD distributions, subtraction image (elderly minus young) and endocortical and pericortical radii from tibial midshaft for both groups. The solid black line represents young men and the grey line elderly men.

For anatomically proper alignment and comparison of bone cross-sections between individuals, the cross-sectional moments of inertia for the two orthogonal axes (i.e., the horizontal and vertical axes of the original pQCT image) were first calculated using Cartesian coordinates as follows:

$$I_x = \sum_{i=1}^{n} y_i^2 dA \quad (5)$$

where x= axis of interest, (horizontal or vertical axis), n= number of pixels, i= index of pixel, y= the perpendicular distance from the axis of interest and dA= area of pixel.

Then to determine the rotation angle needed for the calculation of maximal and minimal cross-sectional moments of inertia, the product moment of area was calculated as:

$$I_{xy} = \sum_{i=1}^{n} x_i y_i dA \quad (6)$$

where n= number of pixels, i= index of pixel, x= horizontal coordinate of the pixel in relation to the area center of mass (the value may be negative), y= vertical coordinate of the pixel in relation to the area center of mass (the value may be negative), and dA= area of pixel.

Finally, the rotation angle needed for rotating the original horizontal and vertical image axes to correspond to maximal and minimal bending axes was obtained as:

$$\alpha = \frac{tan^{-1}\left(\frac{2I_{xy}}{I_x - I_y}\right)}{2} \quad (7)$$

Using this rotation angle, the most posterior sector (#1) and the most anterior sector (#19) could be properly aligned in terms of the axes representing the minimal and maximal cross-sectional moments of inertia.

Validation of the proposed method

To assess the validity of the proposed method a set of synthetic phantom images were created. The validity was assessed by comparing the expected results (i.e. based on synthesised geometry and density) to the ones given by the analysis software. Three sets of synthetic phantom images were created. 1) Synthetic ring phantoms (three phantoms) with varying endosteal radii. 2) Synthetic elliptical phantoms with varying radial density distribution (Figure 2) (nine phantoms) in varying orientations of the ellipse. 3) Synthetic elliptical phantoms with varying polar density distribution in varying orientations of the ellipse (Figure 2) (nine phantoms). In the phantoms with varying density distribution, the density was varied linearly from 820 to 1200 mg/cm$^3$ either from endosteal to periosteal border (i.e. radial phantom) or from -$\pi$ to $\pi$ in polar coordinates (i.e. polar phantom).

Root mean squared coefficients of variation ($CV_{RMS}$) were calculated for repeated measurements of four individuals. The mean $CV_{RMS}$ were: endocortical radii 3.4% (1.5 to 6.0%), pericortical radii 1.5% (0.4 to 3.0%), endocortical sectors 2.4% (0.8 to 5.8%), midcortical sectors 1.4% (0.5 to 2.3%) and pericortical sectors 1.5% (0.5 to 3.4%).

*Application of the proposed method*

Data from 20 young (mean age 24 (SD 2) years, body mass 77 (11) kg, height 178 (6) cm) and 25 elderly (72 (4) years, 75 (9) kg, 172 (5) cm) male volunteers from our database[14] was used in the present study to compare radial and polar cortical vBMD distribution between age groups. Single pQCT (XCT 2000, Stratec Medizintechnik GmbH, Pforzheim, Germany) images (in-plane pixel size 0.8 mm, slice thickness 2.5 mm) from 50% of the tibial length from the distal end plate towards the knee were reanalysed. The difference in density distribution be-

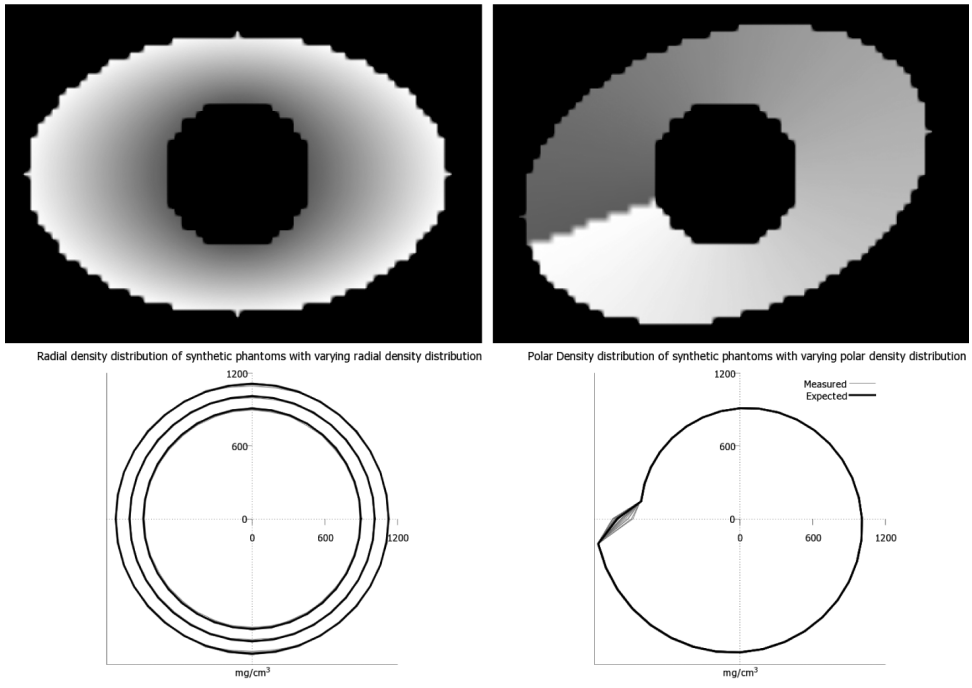


**Figure 2.** Synthetic elliptical phantoms with varying radial (left panel) and polar (right panel) density distribution (density was varied linearly from 820 to 1200 mg/cm$^3$. Upper row: The orientation of the synthetic elliptical phantoms was varied as can be seen between the radial and polar phantoms above. Lower row: The expected values are plotted in black and were calculated from the analytical function used to create the discretized synthetic phantoms. Values from the seven phantoms having orientation varied by less than 45$^o$ overlaid with gray color.

tween the younger and older men was estimated using multivariate analysis of variance (MANOVA) using the division (either thirty six polar sectors or three radial divisions) as a within-subject factor and age group as a between-subjects factor. A statistically significant age group by division/sector interaction was considered to suggest age dependent difference in cortical vBMD distribution. Significant age group differences were considered to suggest different mean vBMD between ages. Statistical analyses were conducted with SPSS 17.0.1 (SPSS Inc.) software and the significance level was set at P≤0.05.

## Results

*Validation*

For bone geometry (cortical area) and strength (polar stress strain index) errors based on the measured and expected results from the three ring phantoms varied from 0.5 to 1.1% and from 0 to 0.5%, respectively. As expected, no error was observed in vBMD, as vBMD is not dependent on the area related errors caused by discretization of the analytical function. The errors in endocortical, midcortical and pericortical sectors varied from 1.0 to 2.0% in the synthetic elliptical phantom with varying radial density distribution (Figure 2). The errors in respective sectors varied from 0.3 to 0.9% in the synthetic elliptical phantoms with varying polar density distribution, when the sector number 19 overlaying an abrupt change in density was excluded from the analysis (Figure 2). The coefficient of variations in the analysed polar and radial density values ranged from 0.05 to 1.15% when the orientation of the ellipse was varied between -40 to 40$^o$. However, if the orientation was varied by more than 45$^o$, the alignment was misclassified by 180$^o$ by the software.

*Application*

For mid-tibial whole bone cortical vBMD, there was no difference between the young and older men (young 1135(16) mg/cm$^3$ vs. older 1130(28) mg/cm$^3$, P=0.696). In the regional analysis, no difference between the age groups was observed for polar vBMD distribution (age group x sector interaction P=0.178), whereas there was a significant age group by division interaction for radial vBMD distribution (P<0.001) (Figure 1). On average, endocortical vBMD tended to be lower in the older compared to younger men [young mean 1170 mg/cm$^3$ 95% CI (1156 to 1184) vs older 1155 mg/cm$^3$ (1142 to 1168)], pericortical higher [young 1210 mg/cm$^3$ (1200 to 1221) vs. older men 1220 mg/cm$^3$ (1211 to 1229)], while no difference was observed at the midcortical division [young 1222 mg/cm$^3$ (1211 to 1234) vs. older men 1218 mg/cm$^3$ (1208 to 1228)].

## Discussion

We demonstrated that the open source analysis approach for evaluating cortical density distribution of peripheral computed tomography images gave expected results, when compared to synthetic phantoms and was effective for detecting regional vari-

ations in volumetric density throughout the mid-tibial cortex as well as differences in regional density between young and elderly men. Specifically, our regional analysis tool captured that cortical vBMD was lowest at the inner endocortical region of the mid-tibia, especially in older men and that the older and younger men differed in the radial density distribution. These findings are as one might have expected looking at age-related porosity changes throughout the bone cortex at appendicular skeletal sites in older adults[1-3]. Furthermore, our regional analysis tool could capture the well known age-related outward expansion and thinning of the cortex during the radii determination step[15]. Contrary to the regional differences in cortical vBMD between young and older men in our study, our conventional analysis of whole bone cortical vBMD found that there were no age differences. These findings seem to indicate that detailed density distribution analysis may provide additional insights into cortical bone adaptations that cannot be obtained from routine analysis of cortical bone applied to pQCT scans.

Several previous studies in children and older adults have examined the effects of growth and exercise on radial and polar cortical vBMD[2,3,13,16-18]. Briefly, the findings from these studies highlight that there are region specific effects of growth and loading on the distrbution of cortical vBMD, with little difference detected in whole bone cortical vBMD. While these findings are consistent with the results from our study, the specific technical details related to the analysis of radial cortical vBMD in these studies was limited. Thus, one of the main aims of this study was to describe in detail how the data from a (p)QCT image file can be read and processed on a pixel per pixel level to quantify radial and polar cortical vBMD.

Open source bone image analysis tools[19,20], built as a ImageJ plug-ins (rsbweb.nih.gov/ij), have been recently introduced*. One of the benefits of open source code is the reduction in workload by being able to reuse old code and thus not needing to reproduce functionality already available. The present approach or its parts can easily be applied to a range of image formats and imaging modalities. The original version of the present analysis method was written in C++ language[21]. However, C++ code needs to be recompiled for each operating system, whereas Java software is portable across operating systems (N.B.: the open source bone analysis based on ImageJ software[20] is also written in Java). Due to the upside of having the source code in Java, we have ported our analysis tool to Java, added the necessary code to use it as an ImageJ plug-in and uploaded the source code (along with the compiled application) to densitydistribution.comli.com. Since the analyses of the BoneJ package do not provide regional bone mineral analysis, the present approach and associated source code complement the growing body of open source bone image analysis methodologies[19,20].

There are several limitations, which should be considered while estimating cortical porosity from computed tomography images. The cortical vBMD analysis of CT images is limited by the resolution of the measurement device and therefore in this paper we can only speculate whether the differences observed in vBMD distributions were related to local mineralization or porosity. The present results, however, are nicely in line with porosity results obtained using methods with higher resolution[1]. Another important decision in density distribution analysis is related to the selection of density thresholds used for segmenting cortex from the images. As recently discussed by Zebaze et al.[1], the selection of threshold will either include or exclude trabecularized cortex at the endosteal surface with obvious consequences. In the present study a high threshold was chosen to exclude the majority of trabecularized cortex from endosteal surface. Furthermore peeling out the innermost and outermost pixel rows was further expected to minimize the potential confounding effect of trabecularization and also minimize partial volume effect at the periosteal surface. Further, since pQCT employs continuous X-ray energy spectrum, the beam hardening effect on density results cannot be ruled out[4]. Although beam hardening effects are minimized with modern measurement systems[22], according to our experimentation (unpublished data), the effect does exist in the device used for the measurements of this study. However, while it is hardly likely that the beam hardening effect would have modulated the present results to considerable extent, the potential effect of beam hardening should not be forgotten when analysing computed tomography data. It should also be noted that the method used for aligning the polar distribution (be it density or radii) results failed, if the alignment of the bone was off by more than 45°. Consequently, at least visual confirmation of the analysis results is mandatory, if polar distribution results are of interest. For radial distribution, the misalignment is of no consequence.

In conclusion, we propose that the assessment of regional cortical vBMD from (p)QCT scans using the open access analysis software described in this paper offers promise as a tool to estimate sector and circumferential differences in cortical density (as an estimate of porosity[8]) in humans.

*Acknowledgements*

*The study was financially supported by the Academy of Finland (# 114925).*

## Appendix

The associated Java source code and compiled software along with a sample pQCT image may be downloaded from densitydistribution.comli.com. The sample image is provided with the explicit approval of the individual from whom the image was taken. The image may be used for any purpose without restrictions.

** Recently, Doube et al.[20] pointed out that there are several advantages in creating open source analysis tools. Firstly, it is a fundamental scientific requirement that a scientist knows the steps taken in producing the results. In other words, using black box analyses should be avoided whenever possible. Secondly, open source tools enable replication of analyses by independent research groups, and thus scientific integrity is improved. Thirdly, open source tools can be tailored to fit the needs of a particular application possibly enabling faster scientific advances, and fourthly they are globally available for scientists with varying economic background.*

## References


1. Zebaze RM, Ghasem-Zadeh A, Bohte A, et al. Intracortical remodelling and porosity in the distal radius and postmortem femurs of women: a cross-sectional study. Lancet 2010;375:1729-1736.
2. Bell KL, Loveridge N, Power J, et al. Regional differences in cortical porosity in the fractured femoral neck. Bone 1999;24:57-64.
3. Goldman HM, Bromage TG, Boyde A, et al. Intrapopulation variability in mineralization density at the human femoral mid-shaft. J Anat 2003;203:243-55.
4. Sievänen H, Koskue V, Rauhio A, et al. Peripheral quantitative computed tomography in human long bones: evaluation of *in vitro* and *in vivo* precision. J Bone Miner Res 1998;13:871-82.
5. Martin RB. Determinants of the mechanical properties of bones. J Biomech 1991;24(Suppl.1):79-88.
6. Bousson V, Bergot C, Meunier A, et al. CT of the middiaphyseal femur: cortical bone mineral density and relation to porosity. Radiology 2000;217:179-87.
7. Basillais A, Bensamoun S, Chappard C, et al. Three-dimensional characterization of cortical bone microstructure by microcomputed tomography: validation with ultrasonic and microscopic measurements. J Orthop Res 2007;12:141-8.
8. Seeman E. Growth in bone mass and size-are racial and gender differences in bone mineral density more apparent than real? J Clin Endocrinol Metab 1998;83:1414-9.
9. Cervinka T, Hyttinen J, Sievänen H. Enhanced bone structural analysis through pQCT image preprocessing. Med Eng Phys 2010;32:398-406.
10. Rittweger J, Michaelis I, Giehl M, et al. Adjusting for the partial volume effect in cortical bone analyses of pQCT images. J Musculoskelet Neuronal Interact 2004;4:436-41.
11. Kontulainen S, Liu D, Manske S, et al. Analyzing cortical bone cross-sectional geometry by peripheral QCT: comparison with bone histomorphometry. J Clin Densitom 2007;10:86-92.
12. Hangartner TN. Thresholding technique for accurate analysis of density and geometry in QCT, pQCT and microCT images. J Musculoskelet Neuronal Interact 2007;7:9-16.
13. Kontulainen SA, Macdonald HM, McKay HA. Change in cortical bone density and its distribution differs between boys and girls during puberty. J Clin Endocrinol Metab 2006;91:2555-61.
14. Rantalainen T, Sievänen H, Linnamo V, et al. Bone rigidity to neuromuscular performance ratio in young and elderly men. Bone 2009;45:956-63.
15. Feik SA, Thomas CD, Bruns R, et al. Regional variations in cortical modeling in the femoral mid-shaft: sex and age differences. Am J Phys Anthropol 2000;112:191-205.
16. Atkinson PJ, Weatherell JA. Variation in the density of the femoral diaphysis with age. J Bone Joint Surg Br 1967; 49:781-8.
17. Lai YM, Qin L, Hung VW, et al. Regional differences in cortical bone mineral density in the weight-bearing long bone shaft-a pQCT study. Bone 2005;36:465-71.
18. Cooper DM, Ahamed Y, Macdonald HM, et al. Characterising cortical density in the mid-tibia: intra-individual variation in adolescent girls and boys. Br J Sports Med 2008;42:690-5.
19. Laskey MA, de Bono S, Zhu D, et al. Evidence for enhanced characterization of cortical bone using novel pQCT shape software. J Clin Densitom 2010;13:247-55.
20. Doube M, Klosowski MM, Arganda-Carreras I, et al. BoneJ: Free and extensible bone image analysis in ImageJ. Bone 2010;47:1076-9.
21. Rantalainen T, Nikander R, Daly RM, et al. Exercise loading and cortical bone distribution at the tibial shaft. Bone 2011;48:786-91.
22. Schneider W, Bortfeld T, Schlegel W. Correlation between CT numbers and tissue parameters needed for Monte Carlo simulations of clinical dose distributions. Phys Med Biol 2000;45:459-78.